Liquid Crystals
Publication details, including instructions for authors and subscription information:
http://www.informaworld.com/smpp/title~content=t713926090

Thermotropic liquid crystals based on chito-oligosaccharides. II. Discotic columnar liquid crystals in chitobiose octaalkanoates and chitotriose hendecaalkanoates

To cite this Article (1992) 'Thermotropic liquid crystals based on chito-oligosaccharides. II. Discotic columnar liquid crystals in chitobiose octaalkanoates and chitotriose hendecaalkanoates', Liquid Crystals, 12: 4, 603 — 611

To link to this Article: DOI: 10.1080/02678299208029096

URL: http://dx.doi.org/10.1080/02678299208029096

LIQUID CRYSTALS, 1992, VOL. 12, NO. 4, 603–611

Thermotropic liquid crystals based on chito-oligosaccharides

II. Discotic columnar liquid crystals in chitobiose octaalkanoates and chitotriose hendecaalkanoates

by M. SUGIURA, M. MINODA, T. FUKUDA, T. MIYAMOTO*
Institute for Chemical Research, Kyoto University,
Uji, Kyoto 611, Japan

and J. WATANABE
Department of Polymer Chemistry, Tokyo Institute of Technology,
Ookayama, Meguroku, Tokyo 152, Japan

(*Received 19 November 1991; accepted 10 March 1992*)

Chitobiose octaalkanoates and chitotriose hendecaalkanoates with varying acyl pendant lengths were synthesized and their mesophase properties studied. Both series of derivatives showed an enantiotropic mesophase in a wide temperature region below 200°C. An X-ray diffraction analysis revealed the mesophase to be of a hexagonal columnar type, in which the columns built up by a periodic stacking of chitobiose or chitotriose cores are packed into a two dimensional hexagonal lattice. The mesophase is thus similar to the hexagonal ordered columnar (D_{ho}) phase in discotics. Compared with cello-oligosaccharide counterparts, the diameter of the column is fairly large and the stacking period somewhat short; these can be interpreted as resulting from the intermolecular hydrogen bonding which is formed between the secondary amide group in the C2 position and the ester group.

1. Introduction

Since the discovery of the first discotic liquid crystals [1], there has been an increasing number of papers reporting the synthesis and mesophase properties of new discogenic compounds [2]. The accepted principle was that a discotic liquid crystal has to contain a flat, rigid, aromatic, and/or disc-shaped core of a high symmetry. However, it has been shown recently that non-aromatic and/or non-flat molecules with a lower symmetry can also form a discotic mesophase [2, 3]. During the course of a series of studies on poly- and oligosaccharide-based liquid crystals, we have found that some *D*-cellobiose derivatives, in which all the hydroxyl groups are blocked with long alkyl chains via an ester linkage, can form a hexagonal ordered columnar (D_{ho}) phase in a class of discotics [4]. In addition, the discotic columnar phase has also been observed for peracylated glycosides and cellobiosides [5]. Quite recently, we succeeded in the synthesis of acylated chito-oligosaccharides, i.e. chitobiose octaalkanoates and chitotriose hendecaalkanoates, and confirmed that they also exhibit a stable thermotropic mesophase, perhaps a discotic columnar phase [6]. These derivatives are distinguished from the cello-oligosaccharide equivalents by the presence, at the C2 position of the glucopyranose unit, of a secondary amide group (see figure 1), which is expected to bring about a rather strong intermolecular interaction, i.e. hydrogen

---

* Author for correspondence.

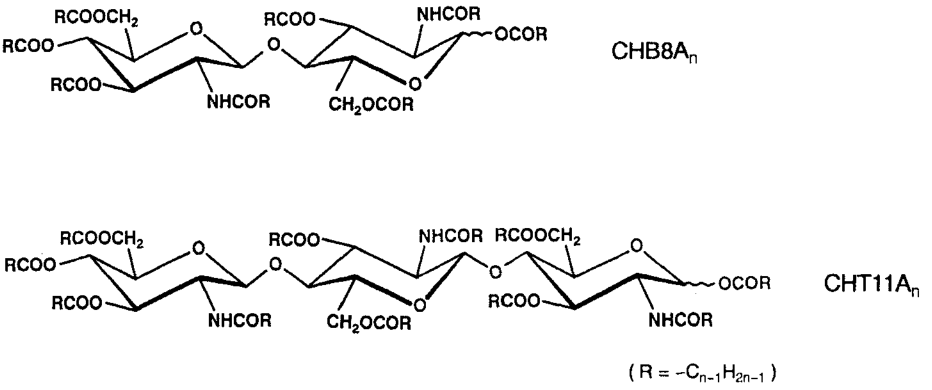

Figure 1. Structures of acylated chito-oligosaccharides.

bonding, thereby affecting the mesophase properties. In this paper, we report the results of calorimetric, optical microscopic, and X-ray investigations of the chito-oligosaccharide derivatives, and give evidence of their type of discotic columnar mesophase. Furthermore, by comparison with the cello-oligosaccharide equivalents we examine the effect of the secondary amide groups of these derivatives on the mesophase properties.

2. Experimental

2.1. *Materials*

The compounds used in this study, *N*,O-acylated chitobiose and chitotriose are abbreviated as CHB8A$_n$ and CHT11A$_n$, respectively, in which n ($n=6$, 10, 14, and 18) refers to the number of carbon atoms in the acyl pendant (see figure 1). They were prepared by the acylation of chitobiose and chitotriose with corresponding fatty acid chlorides in chloroform/pyridine. Chitobiose and chitotriose (Seikagaku Kogyo Co., Ltd.) were obtained as a hydrochloric acid salt and employed without further purification. The acid chlorides (Tokyo Kasei Kogyo Co., Ltd.) were used as received. Chloroform and pyridine (Nacalai Tesque, Inc.) were distilled over calcium hydride prior to use.

In a typical preparation, chitobiose hydrochloride (200 mg; 0·59 mmol) was soaked in pyridine (10 ml) overnight and then the pyridine was evaporated off under reduced pressure. The liberated chitobiose was dispersed in a mixture of pyridine (20 ml) and chloroform (20 ml) with stirring. To this solution, myristoyl chloride (1·6 ml; 10 equivalents based on the chitobiose) was added dropwise at room temperature. After an hour of the reaction, the solution was poured into methanol, filtered and reprecipitated with diethyl ether. In the case of the derivatives with short side chains (CHB8A$_6$, CHB8A$_{10}$ and CHT11A$_6$) the product was purified by preparative size exclusion chromatography and then recrystallized. All products were epimeric mixtures containing over *c.* 95 per cent of the α-anomer [6]. Further details of the synthesis and characterization of these compounds were described previously [6].

2.2. *Measurements*

The thermal phase behaviour was studied by differential scanning calorimetry (DSC) on a Rigaku Denki Model DSC-8230, Japan, at a constant heating/cooling rate of 10°C min^{-1}. The optical microscopy was performed on a Nikon Model Optiphoto-

Pol, Japan, employing a Mettler Model FP 82 hot stage, Switzerland. X-ray diffraction patterns from samples in glass capillaries were recorded at different mesophase temperatures, using Ni-filtered Cu–K_α radiation. The sample temperatures were regulated by a Mettler Model FP 80 hot stage.

3. Results and discussion

From differential scanning calorimetry (DSC), both $CHB8A_n$ and $CHT11A_n$ with $n=10$, 14 and 18 were found to show a thermotropic mesophase in both heating and cooling modes, i.e. they are enantiotropic liquid crystals. When the acyl length was too short, the melting temperature of the sample was so high (> 200°C) that decomposition took place before melting. Specifically, $CHB8A_6$ and $CHT11A_6$ were significantly decomposed, and so, their mesophase properties could not be elucidated.

On the basis of the cooling DSC thermograms, two transition temperatures were determined. The lower transition, T_m, corresponds to the melting of the crystals to a

Table 1. Transition temperatures obtained for $CHB8A_n$ and $CHT11A_n$.

Product	T_m	T_i
$CHB8A_{10}$	65°C	207°C
$CHB8A_{14}$	70°C	196°C
$CHB8A_{18}$	73°C	185°C
$CHT11A_{10}$	60°C	195°C
$CHT11A_{14}$	65°C	175°C
$CHT11A_{18}$	75°C	170°C

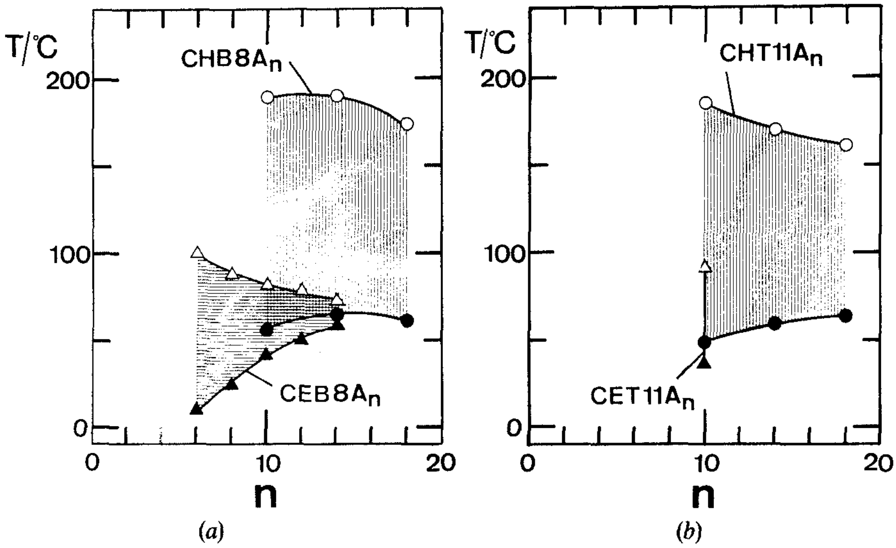

Figure 2. Transition temperatures as a function of the number of the total carbon atoms in the acyl pendant (*n*). (*a*) $CHB8A_n$, (*b*) $CHT11A_n$. (○), isotropization point, T_i; (●), melting point, T_m. The corresponding transition temperatures are also plotted by the triangles, observed for $CEB8A_n$ and $CET11A_n$.

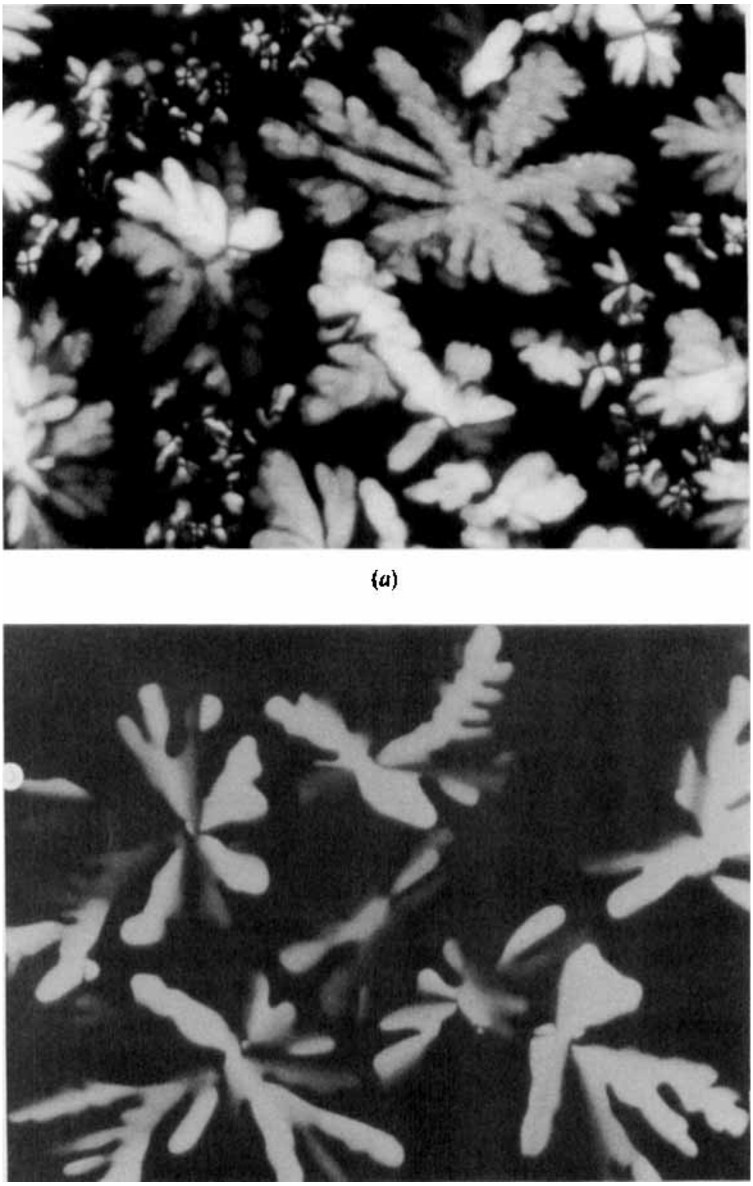

(*a*)

(*b*)

Figure 3. Optical microscopic textures of the anisotropic nucleation germs appearing on very slow cooling from the isotropic liquid: (*a*) $CHB8A_{10}$; (*b*) $CEB8A_{10}$.

mesophase, and the higher one, T_i, to the isotropization of the mesophase. These transition temperatures are listed in table 1. In figure 2 (*a*), T_m and T_i for $CHB8A_n$ are plotted as a function of *n*, the number of carbon atoms in the acyl pendant. Figure 2 (*b*) shows similar plots for $CHT11A_n$. All these compounds exhibit a mesophase in nearly the same temperature region between 50 and 200°C, even though the temperature range becomes somewhat narrower with an increase of *n*.

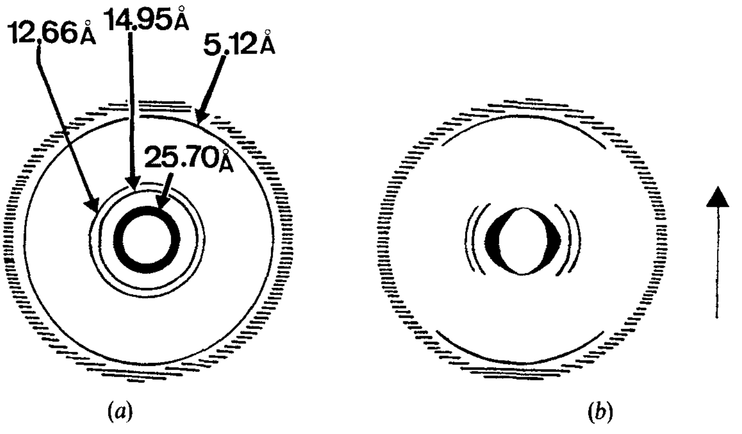

Figure 4. X-ray diffraction patterns of the mesophase of CHB8A$_{14}$ obtained (*a*) before and (*b*) after shearing at 100°C. A shear was applied in the direction indicated by the arrowhead.

Table 2. X-ray data obtained for the mesophase of CHB8A$_n$ and CHT11A$_n$ at 100°C.

Product	d_{obs}/Å (100)	(110)	(200)	Meridional	Calculated density/g ml^{-1}
CHB8A$_{10}$	22·2	12·9	—	5·15	0·89
CHB8A$_{14}$	25·7	14·9	12·7	5·12	0·84
CHB8A$_{18}$	27·9	16·3	14·2	5·13	0·86
CHT11A$_{10}$	25·2	14·2	—	5·15	0·87
CHT11A$_{14}$	28·9	16·7	14·5	5·11	0·94
CHT11A$_{18}$	31·6	18·5	15·8	5·12	0·94
CEB8A$_{10}$	20·8	12·1	10·4	5·40	0·95
CET11A$_{10}$	24·5	14·0	—	5·40	0·98

All specimens exhibited characteristic mesomorphic textures under a polarization microscope when the temperature was slowly cooled from the isotropic phase. On cooling, small birefringent circular germs at first appeared and immediately grew to form the characteristic leaf and flower-like texture, such as shown by CHB8A$_{10}$ (see figure 3 (*a*)). The texture and its growth were essentially similar to those observed for the cello equivalent, CEB8A$_{10}$ (see figure 3 (*b*)), indicating that this mesophase is classified as the same type as that of the cello version, i.e. discotic columnar phase [4].

Precise determination of the mesophase structures of CHB8A$_n$ and CHT11A$_n$ could be performed by X-ray diffraction. In figure 4 (*a*), a typical diffraction pattern obtained for CHB8A$_{14}$ at 100°C is illustrated. Three sharp diffraction rings can be seen at small angles, which correspond to real spacings of 25·70 Å, 14·95 Å, and 12·66 Å, respectively, the ratios being very close to $1 : 1/3^{1/2} : 1/2$. In addition, the sample oriented by shearing gives a different diffraction pattern, in which all of the reflections at small angles lie on the equatorial line perpendicular to the shearing direction (see figure 4 (*b*)). These results are consistent with the expected structure, namely a discotic columnar mesophase with a hexagonal packing of the columns. The Bragg spacings of the

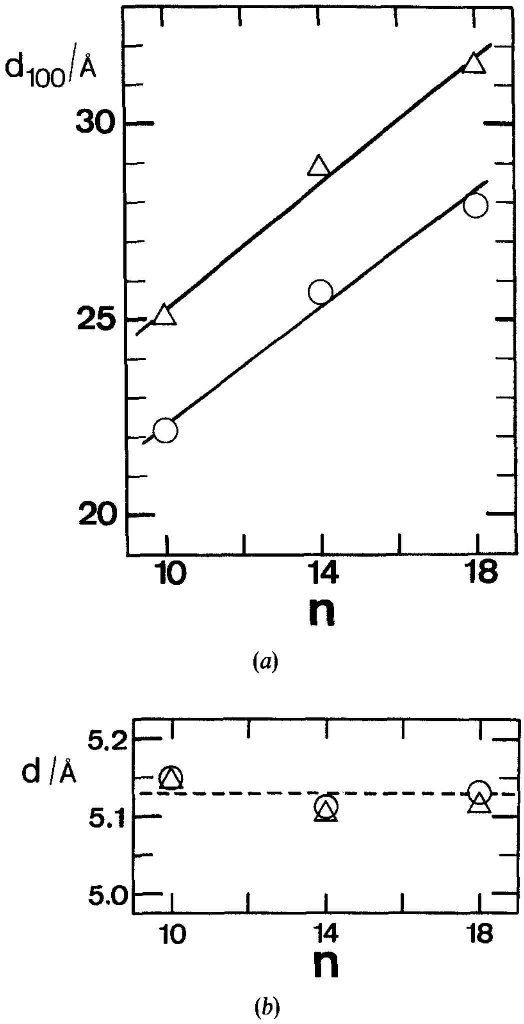

Figure 5. Plots of (*a*) the lattice spacing of the 100 reflection and (*b*) the periodicity along the column axis versus the total number, *n*, of carbon atoms in the acyl pendant. ○, CHB8A$_n$; △, CHT11A$_n$.

reflections observed for other CHB8A$_n$ and CHT11A$_n$ specimens are listed in table 2. The same packing features as previously described were found for all of them. In figure 5 (*a*), the lattice spacing of the 100 reflection (recorded at 100°C), which is a measure of the diameter of the column, is plotted against *n*. For both CHB8A$_n$ and CHT11A$_n$, the spacing increases in direct proportion to *n*. For the same *n*, the spacing of CHT11A$_n$ is larger than that of CHB8A$_n$.

The X-ray pattern of the oriented specimen shown in figure 4 includes another significant reflection on meridional line, which reflects an ordered packing of molecules within a column. The spacing of this reflection, corresponding to the intermolecular distance along the column axis, is listed in table 2 and also plotted as a function of *n* in figure 5 (*b*). Interestingly, the distance remains constant at around 5·1 Å for all *n*, indicating that neither the acyl length nor the size of the core oligosaccharide influences the packing period along the columns. A further insight into the molecular packing can be gained by the evaluation of the mesophase density. The column cross-sectional area S is given by $S=a^2(\sqrt{3}/2)$, where a is the side length of the two-dimensional hexagonal lattice (see table 2). Irrespective of the size of the central core, the periodicity along the column was 5·1 Å; hence, the volume of a unit lattice is $5{\cdot}1S$. Assuming that one molecule is included in this unit volume, we can calculate the specific gravities to be about $0{\cdot}9\,\mathrm{g\,ml^{-1}}$ for both CHB8A_n and CHT11A_n, as shown in table 2. In light of the expected specific gravity values and also those calculated for other hexagonal mesophases of similar chemical compositions [3 (*b*), 4, 7], these values appear very plausible.

The mesophase structure deduced from the mentioned results is schematically presented in figure 6. It can be classified into the same hexagonal ordered columnar (D_{ho}) phase as observed for the cello–oligo equivalents, in which the columns built up by a periodic stacking of the chitobiose or chitotriose moieties with the normals of the glucopyranose rings arranged parallel to the column axis are packed into a two dimensional hexagonal lattice.

Compared with the cello counterparts, however, the chito derivatives exhibit two remarkable characteristics from their mesophase structure and properties. One concerns the mesophase temperature region. As figure 2 shows, the isotropization temperatures of the chito derivatives (150–200°C) are appreciably higher than those of the cello counterparts (80–100°C), while the melting temperatures are in the same range. This means that the columnar mesophases of the chito derivatives are much more stabilized than those of the cello derivatives. The second characteristic is relevant to the intermolecular spacing along the column; this spacing of the chito derivatives is 5·1 Å, which is considerably smaller than the value of 5·4 Å for the cello derivatives. Thus the chito derivatives assume a closer packing of molecules along the column. Furthermore, the alkyl side chains of the chito derivatives seem to be somewhat more extended than those of the cello equivalents: for example, the column diameter of CHB8A_{10} was found to be 25·6 Å, while that of CEB8A_{10} was 24·0 Å [4].

Chemically, the chito derivatives are distinguished from the cello equivalents only by the existence of an amide group at the C2 position of the glucopyranose unit. Hence,

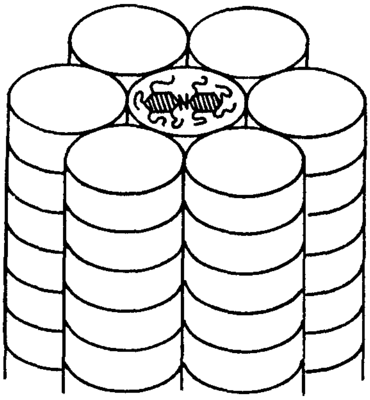

Figure 6. Structure of the discotic columnar (D_{ho}) phase of CHB8A_n. Here, the columns are composed of the regular stacking of the chitobiose moiety and packed into a two dimensional hexagonal lattice.

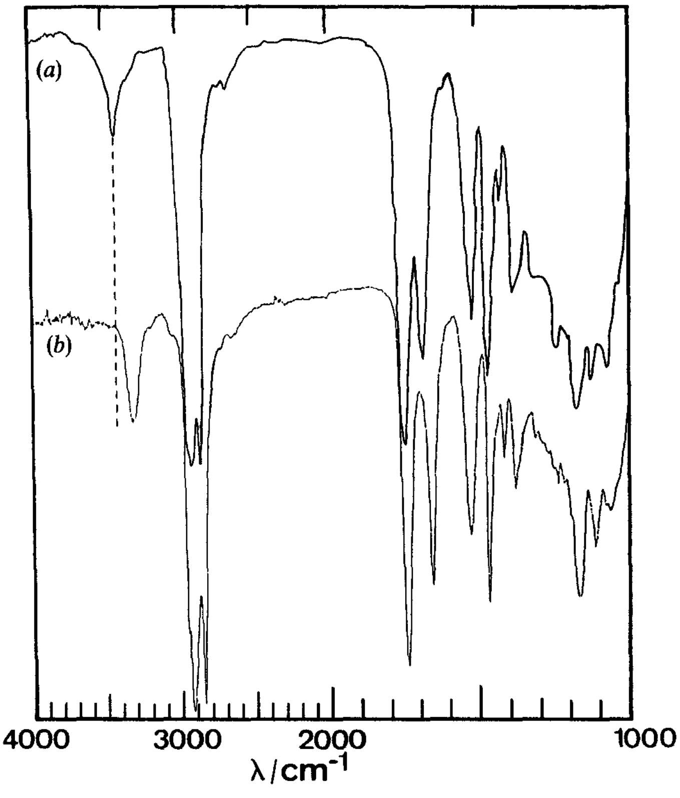

Figure 7. Infrared spectra of CHT11A$_{18}$ in (*a*) chloroform solution and (*b*) the bulk (quenched from mesophase).

the mentioned characteristics can be attributed to intermolecular hydrogen bonding, possibly between the amide and ester groups. In order to clarify this, IR measurements were carried out for undiluted CHT11A$_{18}$ as well as its dilute chloroform solution. The undiluted (bulk) sample was prepared by quenching from the mesomorphic temperature. The IR spectra thus obtained are shown in figure 7. The material in solution exhibits the N–H stretching absorption at 3422 cm^{-1}. This frequency value is normally observed for amide groups which experience no hydrogen bonding [8]. On the other hand, the corresponding absorption for the bulk specimen appears at 3329 cm^{-1}. Obviously the band has shifted to a lower frequency, confirming hydrogen bonding in the bulk. On the basis of an empirical relationship [8], the hydrogen bond distance, N–H...O, was estimated to be about 3·0 Å. Particularly interesting is the fact that despite the fairly anisotropic shapes of the mesogenic central cores, the chito-oligosaccharide alkanoates studied here do form the discotic columnar phase with hexagonal symmetry. The important question is now raised as to whether or not homologous alkanoates of higher degrees of polymerization, such as tetrasaccharide and pentasaccharide derivatives, can also form the same type of mesophase. If so, how can those highly asymmetric compounds with a large axial ratio stack themselves into a symmetrical column? It is also important to note that carbohydrates can potentially undergo many types of regio- and/or stereo-selective reactions, hopefully providing a number of new mesogenic derivatives with a variety of structures. In progress are studies on the synthesis and mesophase properties of other carbohydrate-based liquid crystals.

References

[1] CHANDRASEKHAR, S., SADASHIVA, B. K., and SURESH, K. A., 1977, *Pramana*, **9**, 471.

[2] For a review, see CHANDRASEKHAR, S., and RANGANATH, G. S., 1990, *Rep. Prog. Phys.*, **53**, 57.

[3] (a) CARFAGNA, C., IANNELLI, P., ROVIELLO, A., and SIRIGU, A., 1987, *Liq. Crystals*, **2**, 611. (b) MALTHETE, J., COLLET, A., and LEVELUT, A. M., 1989, *Liq. Crystals*, **5**, 123. (c) LEVELUT, A. M., MALTHETE, J., and COLLET, A., 1986, *J. Phys., Paris*, **47**, 351. (d) ZIMMERMANN, H., POUPKO, R., LUZ, Z., and BILLARD, J., 1988, *Liq. Crystals*, **3**, 759. (e) LATTERMANN, G., 1990, *Molec. Crystals Liq. Crystals*, **182B**, 299.

[4] ITOH, T., TAKADA, A., FUKUDA, T., MIYAMOTO, T., YAKOH, Y., and WATANABE, J., 1991, *Liq. Crystals*, **9**, 221.

[5] (a) VILL, V., and THIEM, J., 1991, *Liq. Crystals*, **9**, 451. (b) ZIMMERMANN, R. G., JAMESON, G. B., WEISS, R. G., and DEMAILLY, G., 1985, *Molec. Crystals Liq. Crystals Lett.*, **1**, 183. (c) TAKADA, A., MA, Y.-D., FUKUDA, T., and MIYAMOTO, T., 1990, *Bull. Inst. Chem. Res. Kyoto Univ.*, **68**, 21.

[6] SUGIURA, M., MINODA, M., FUKUDA, T., and MIYAMOTO, T., 1992, *Bull. chem. Soc. Japan* (in the press).

[7] LEVELUT, A. M., MALTHETE, J., DESTRADE, C., and TINH, N. H., 1987, *Liq. Crystals*, **2**, 877.

[8] PIMENTEL, G. C., and SEDERHOLM, C. H., 1956, *J. chem. Phys.*, **24**, 639.